Available online at www.sciencedirect.com
SCIENCE DIRECT®
Vibrational Spectroscopy 37 (2005) 111–121
VIBRATIONAL SPECTROSCOPY
www.elsevier.com/locate/vibspec

Development of the partial least squares models for the interpretation of the UV resonance Raman spectra of lignin model compounds

Anna-Maija Saariaho[a,*], Dimitris S. Argyropoulos[b], Anna-Stiina Jääskeläinen[a], Tapani Vuorinen[a]

[a]*Laboratory of Forest Products Chemistry, Helsinki University of Technology, P.O. Box 6300, FIN-02015 HUT Espoo, Finland*
[b]*Department of Wood and Paper Science, North Carolina State University, Raleigh, NC 27695-8005, USA*

Received 6 May 2004; received in revised form 29 July 2004; accepted 3 August 2004
Available online 2 December 2004

Abstract

Partial least squares (PLS) modeling was utilized for the interpretation of the ultraviolet resonance Raman (UVRR) spectra of various lignin model compounds. Lignin model compounds presented different structural characteristics of the naturally existing lignin biopolymer within wood materials. The model compounds were grouped according to their monomer type, condensed and conjugated structures. Condensed structures were defined as those having a side group at C5 carbon of the aromatic units. Conjugated model compounds were further subdivided into C=C and C=O as well as stilbene structures. PLS modeling was applied to find the characteristic Raman signals of each structure: *p*-hydroxyphenyl showed characteristic Raman bands at 1488, 1405, 1338, 1215, 1164, 1094, 861–841, 644 cm^{-1}, guaiacyl at 1520, 1285–1270, 1186, 1124, 1078, 1024, 920, 784, 761, 711 cm^{-1}, syringyl at 1588, 1510, 1331, 1228, 1148, 1108, 964, 810, 741 cm^{-1} condensed structures at 1618, 1558, 1492, 1375–1355, 1328, 1223, 975 cm^{-1}, conjugated C=C at 1658, 1538, 1475, 1311, 1215, 1130–1114, 974 cm^{-1}, conjugated C=O at 1695–1662, 1084 cm^{-1} and stilbenes at 1638, 1515, 1435–1421, 1263, 1191, 877, 768 cm^{-1}. The loadings line spectra of different PLS models were further compared with the UVRR spectra of model compounds and hence, the feasibility of PLS modeling was verified. To the best of our knowledge, this is the first time when PLS modeling has been utilized in this manner for the interpretation of such spectra. The defined characteristic Raman bands can further be utilized for the interpretation of UVRR spectra of polymeric lignin samples. PLS models introduce new possibilities for the interpretation of Raman spectra since the UVRR spectral data of complex lignin samples contain broad bands which are cumbersome to fully identify.

Keywords: Condensed structures; Conjugated structures; Lignin model compounds; Monomer type; Partial least squares model; UV resonance Raman spectroscopy

1. Introduction

Lignin, the second most abundant biopolymer on the planet, is a heterogeneous material imparting strength and rigidity to wood by effectively gluing the wood cells together. It is composed of phenylpropane units in an irregular way and hence, its chemical structure is very complex [1]. For the paper production, the wood chips are initially defibrated in chemical pulping thus decreasing the lignin content of the resulting fibers. After defibration, the pulp is further bleached to lower lignin contents. The initial steps in the removal of lignin are rather easy to perform but further bleaching of the delignified pulp could be challenging. This is mainly because the residual lignin on the fiber contains resistant interunit linkages, it is of rather high molecular weight and it also contains strong chemical bonds between lignin and polysaccharides of the wood cell wall. Hence, even fully bleached pulps contain about 0.1 wt.% of residual lignin. The residual lignin is one of the

* Corresponding author. Fax: +358 9 451 4259.
E-mail address: anna-maija.saariaho@hut.fi (A.-M. Saariaho).

0924-2031/$ – see front matter © 2004 Elsevier B.V. All rights reserved.
doi:10.1016/j.vibspec.2004.08.001

key factors in the yellowing of the paper and hence, knowledge on its chemical structure is of great interest and significance to bleaching operations worldwide.

The characterization of the chemical structure of residual lignin is a demanding task. Most of the analytical techniques require its isolation. However, complete and totally representative residual lignin isolation is not possible, since lignin is bound to wood polysaccharides and its isolation procedures might alter its chemical structure [2]. Consequently, since the isolation of lignin has its drawbacks, its analysis should ideally be performed in situ with sensitive and selective analytical tools. Ultraviolet resonance Raman (UVRR) spectroscopy makes the direct characterization of lignin possible even from fully bleached pulps, where only trace amounts of lignin are present [3–5]. The Raman signals of aromatic and unsaturated lignin structures are resonantly enhanced about 10^4 to 10^7 times [6] because these structures absorb light in the UV region. Other wood components, such as polysaccharides do not absorb UV radiation and hence their Raman signals are rather low in intensity. Therefore, Raman signals arising from matrix components are not overwhelming and the detection of lignin vibrations is possible.

Even though lignin can be easily analyzed with UVRR spectroscopy from pulps, the following difficulty lies in the interpretation of the UVRR spectra. A wide range of the chemical structures in the sample has an impact on the resolution of Raman bands. The Raman band originating from the symmetric aromatic vibrational stretching mode of lignin at 1605 cm^{-1} is easily detected [7,8] but other information pertaining to detailed chemical structures remains easily unresolved. Therefore, additional resourceful data handling methods are of great importance. One such method is multivariate data analysis which is rather powerful in detecting similarities in the spectra and in grouping similar datasets into subgroups [9]. Principal component analysis (PCA) compares the dataset effectively and resolves the most important components to be those with highest variability in the variables. Partial least square (PLS) utilizes the principle of comparing *X* and *Y* variables simultaneously and resolves those *X* variables that correlate with *Y*.

In our earlier work we showed that the monomer type (*p*-hydroxyphenyl, guaiacyl and syringyl lignin structures) can be visually detected from the UVRR spectra of extracted wood samples [7]. However, we have found that the interpretation of the UVRR spectra is not as straightforward in most other cases. Therefore, the aim of this study was to investigate whether the multivariate data analysis would be powerful enough in the interpretation of the UVRR spectra of lignin model compounds representing three structures: (A) monomer type (*p*-hydroxyphenyl, guaiacyl and syringyl), (B) C5 condensed and (C) conjugated structures (Fig. 1). A multivariate data analytical approach was selected because it holds the possibility to expand the model further into a quantitative description by which different lignin structures could most likely be quantified. Further scope of the work was to determine characteristic wavenumbers of different lignin structures with a PLS model.

2. Experimental

2.1. Materials

Model compounds were divided into three groups representing (A) monomer type (*p*-hydroxyphenyl, guaiacyl and syringyl), (B) condensed and (C) conjugated structures. The structures and the names of the model compounds are shown in Fig. 1. The condensed structures were defined as those containing substitution at the C5 carbon in the guaiacyl units. Hence, the condensation degree (presented in parentheses in Fig. 1B) varies in the dimeric condensed model compounds. The monomeric model compounds were commercially purchased: 4-methyl-phenol (99% purity), 4-hydroxybenzaldehyde (98%), 4-methylanisole (99%), 4-methyl-2,6-dimethoxyphenol (97%), 3,5-dimethoxy-4-hydroxybenzaldehyde (98%), 3,4,5-trimethoxytoluene (97%), 4-hydroxy-acetophenone (99%) and 3-(4-hydroxy-3-methoxyphenyl)-2-propenal (98%) were purchased from Aldrich Co., 2-methoxy-4-methylphenol (>98%), 3,4-dimethoxytoluene (>97%), 2-methoxy-4-propenyl-phenol (∼95%) and 4-(2-hydroxyethenyl)-2-methoxy-phenol (>97%) from Fluka, 4-hydroxy-3-methoxybenzaldehyde from Schering-Kahlbaum A.G. Berlin, 4-hydroxy-3-methoxy-acetophenone from Johnson Matthey Alfa Products and 4,4′-dihydroxystilbene from ICN Biomedicals Inc., 4-hydroxy-3,3′,4′-trimethoxystilbene was synthesized [10]. Group B model compounds were synthetically produced; 2,2′-dihydroxy-3,3′-dimethoxy-5,5′-diformylbiphenyl [11], 2,4′-dihydroxy-3,3′-dimethoxy-5-methyldiphenylmethane [12], 4-hydroxy-3,3′,4′-trimethoxy-benzophenone [13] and 2,2′-dihydroxy-3,3′-dimethoxy-5,5′-dimethyldiphenylmethane [13,14]. Spectroscopic grade potassium bromide was purchased from Merck.

2.2. Methods

UV resonance Raman spectra were collected with a Renishaw 1000 UV Raman spectrometer equipped with a Leica DMLM microscope and an Innova® 90C FreD™ frequency doubled Ar^+ ion laser (Coherent Inc., California). The excitation wavelengths applied were 244 and 257 nm. The output power of the laser was adjusted to 20 mW and the laser beam was attenuated with a neutral density filter of 10% transmittance. Thereafter, the beam was reflected by mirrors to a 244 or 257 nm dielectric edge filter (Kaiser Optical Systems), which are specific for Stokes lines over 500 cm^{-1}. The beam was further directed to the microscope equipped with deep UV LMU-15X or LMU-40X (OFR Inc., USA) objectives. Due to losses in the light path, the final power at the

sample level was about 1.3 mW with all of the excitation wavelengths. The laser power at the sample level was selected to be as low as possible in order to prevent any undesirable irradiation induced changes or degradation in the sample. Furthermore, during the measurement, the samples were rotated (6 rpm) concentrically (offset 2–3 mm) to average the spectra and to minimize changes in the sample due to the sharply focused UV radiation. Before the measurements the samples were studied for possible degradation reactions by comparing sequentially

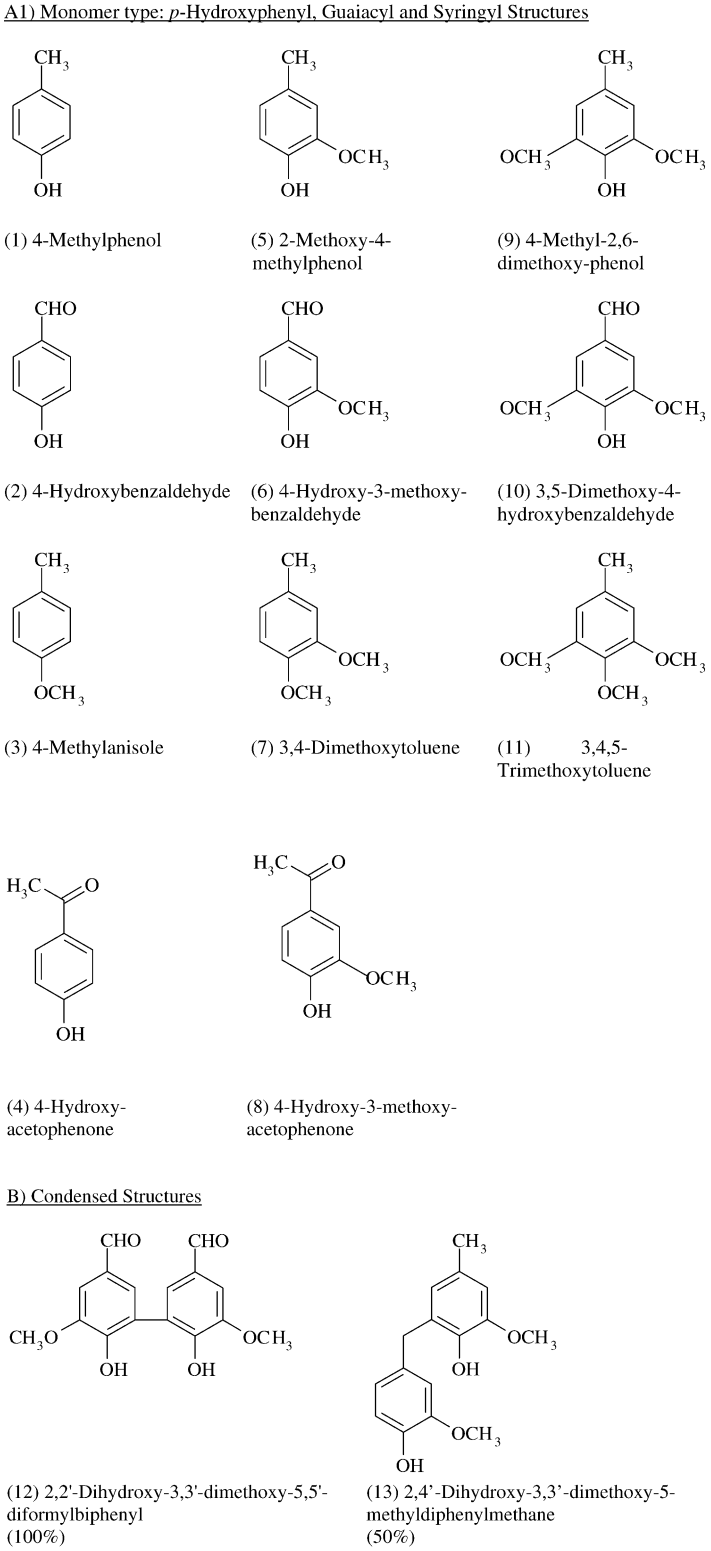

Fig. 1. Chemical structures of the studied model compounds.

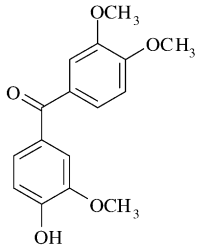

(14) 4-Hydroxy-3,3',4'-trimethoxy-benzophenone
(0%)

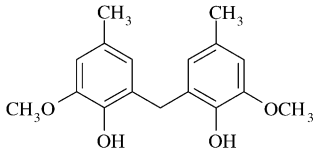

(15) 2,2'-Dihydroxy-3,3'-dimethoxy-5,5'-dimethyldiphenylmethane
(100%)

C) Structures with conjugated double bond (only C=C)

1) Monomers

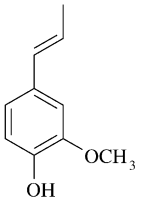

(16) 2-Methoxy-4-propenyl-phenol

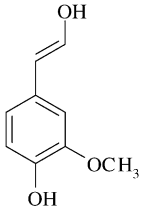

(17) 4-(2-Hydroxyethenyl)-2-methoxy-phenol

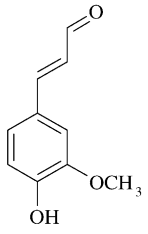

(18) 3-(4-Hydroxy-3-methoxyphenyl)-2-propenal

2) Stilbenes

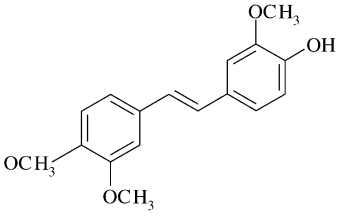

(19) 4-Hydroxy-3,3',4'-trimethoxystilbene

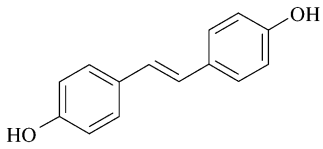

(20) 4, 4' – Dihydroxystilbene

Fig. 1. (*Continued*).

collected spectra and no changes were observable. The backscattered Raman light was passed through the microscope to the edge filters and was further focused on a 50 μm slit by an additional lens. The transmitted Raman light was reflected by a prism mirror to a diffraction grating of 3600 grooves/mm and finally to a UV-coated, deep depletion CCD camera. The spectral data from the CCD camera was processed with GRAMS/32® (Galactic Industries Corporation) software. The spectral range was 500–2000 cm^{-1} and the resolution about 7 cm^{-1}. The upper limit of the spectral range was selected to be 2000 cm^{-1} because the UVRR spectra of wood and lignin samples did not show resonance enhanced signals in 2000–3000 cm^{-1} region.

Table 1
The quantification of the structures of lignin model compounds

Model compound (numbers refer to Fig. 1)	*p*-Hydroxyphenyl	Guaiacyl	Syringyl	C5 condensed	C=O conjugated	C=C conjugated	Stilbenes
1	10	0	0	0	0	0	0
2	10	0	0	0	10	0	0
3	10	0	0	0	0	0	0
4	10	0	0	0	10	0	0
5	0	10	0	0	0	0	0
6	0	10	0	0	10	0	0
7	0	10	0	0	0	0	0
8	0	10	0	0	10	0	0
9	0	0	10	0	0	0	0
10	0	0	10	0	10	0	0
11	0	0	10	0	0	0	0
12	0	10	0	10	10	0	0
13	0	10	0	5	0	0	0
14	0	10	0	0	5	0	0
15	0	10	0	10	0	0	0
16	0	10	0	0	0	10	0
17	0	10	0	0	0	10	0
18	0	10	0	0	0	10	0
19	0	10	0	0	0	0	10
20	10	0	0	0	0	0	10

Solid lignin model compounds were mixed with KBr and pressed at 100 kN to a pellet with a hydraulic press (Perkin Elmer). The amount of model compound in the KBr matrix varied in the range 10–30 mg and that of KBr was about 250 mg. UVRR spectra of pure liquid model compounds were measured in a small cup covered with a quartz glass. Spectral data collection times were varied from 2 to 4 min depending on the intensities of Raman signals and the magnitude of the resonance enhancement. In some cases, a few successive spectra were summed up to improve the signal-to-noise ratio.

Multivariate data analysis was performed on Simca P-8.01 (Umetrics, Sweden) software. The *X* matrix of the PLS models were the spectral data of all 20 model compounds between 2243 cm^{-1} and 391 cm^{-1}, containing totally 556 spectral data points. The *X* matrix, i.e. all model compound spectra, was scaled between 0 and 10, so that the baselines were forced to 0 and the highest intensity band was forced to 10. The highest intensity band in most of the model compound spectra was the aromatic band at about 1600–1620 cm^{-1}. The model compounds **7** and **11** had the highest intensity bands at 760 and 1333 cm^{-1}, respectively. There may be some low intensity bands overlapping at these wavelengths that may bring some inaccuracy to the model. This contribution should, however, be relatively insignificant and it has an impact only on quantitative results, if the model is used for such purpose in the future. The *Y* matrix contained the quantity of the different lignin model compound structures (all together 7 *Y* variables) which were given values 0, 5 and 10 (see Table 1). The values describe the relative quantity of each structure in one aromatic unit. Hence, for monomeric model compounds the value 0 means that there is no such structure in that model compound whereas value 10 describes that the aromatic unit contains the corresponding structure. For dimeric model compounds, 0 means that there is no such structure in either aromatic units, and 10 means that both of the aromatic units contain the structure. Value 5 means that the other aromatic unit of a dimeric model compound contains the corresponding structure whereas the other unit does not. This way both of the *X* and *Y* matrices had variances between 0 and 10.

3. Results and discussion

Because the UVRR spectra of the lignin model compounds were quite complicated, a PCA model was not powerful enough in detecting all of the model compound groups and their characteristic Raman bands. Therefore, the sub-structures of the model compounds were quantified arbitrarily in order to create a model that utilizes the partial least square (PLS) principle. The model compares the given *Y* values (the quantity of a structure) and the *X* variables (spectrum) and finds more easily those *X* variables that are related with a given *Y* value. Hence, the model is more powerful in grouping the samples as well as in detecting the most important Raman bands of different model compound groups. The quantified sub-structures of each model compound are listed in Table 1.

The aromatic structure of all lignin model compounds shows a resonantly or pre-resonantly enhanced Raman band at 1605 cm^{-1} which is due to its symmetric vibrational stretching mode [15]. In principle, a complex PLS model could be composed to predict all sub-structures in compounds simultaneously. After testing of several models it was found that the simple ones worked best and that the characteristic bands within each model compound group were similar and rather independent of bands in the other

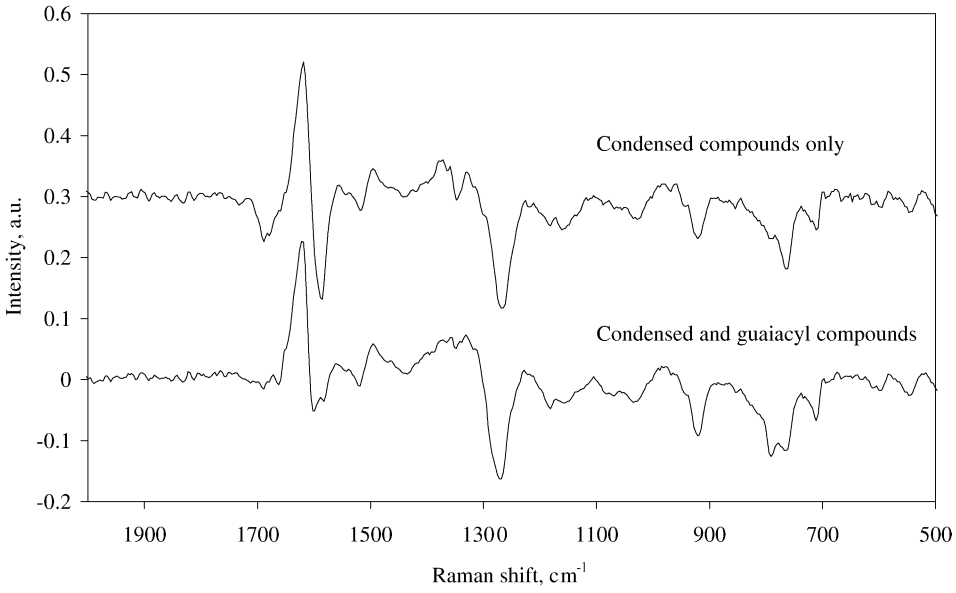

Fig. 2. Two loadings line spectra of C5 condensed structures with two differently formed PLS models. The model with only condensed structures (the upper spectrum) contained the compounds **12**–**15** and the model with condensed and guaiacyl structures (the lower spectrum) contained the compounds **5**–**8** and **12**–**15**.

groups of model compounds. This is illustrated in Fig. 2, in which loadings line spectra of C5 condensed structures are shown from two different PLS models. The first PLS model was composed of group B model compounds only whereas the other model contained also some monomers with the uncondensed guaiacyl structure. The loadings line spectra are relatively similar in both models.

The modeling was tested with both excitation wavelengths (244 and 257 nm) that were available to us, but here we present only the results obtained at 257 nm because the characteristic vibrations were more intense at this wavelength. The characteristic vibrational bands of different lignin model compound structures were also similar at both wavelengths. However, the fluorescence background might disturb the analysis in some cases when excited with 257 nm. This is because the excitation wavelength is closer to visible region where the fluorescence background is often a hindrance. The fluorescence is not necessarily detected with model compounds but sometimes it can be a disturbing factor with real lignin samples.

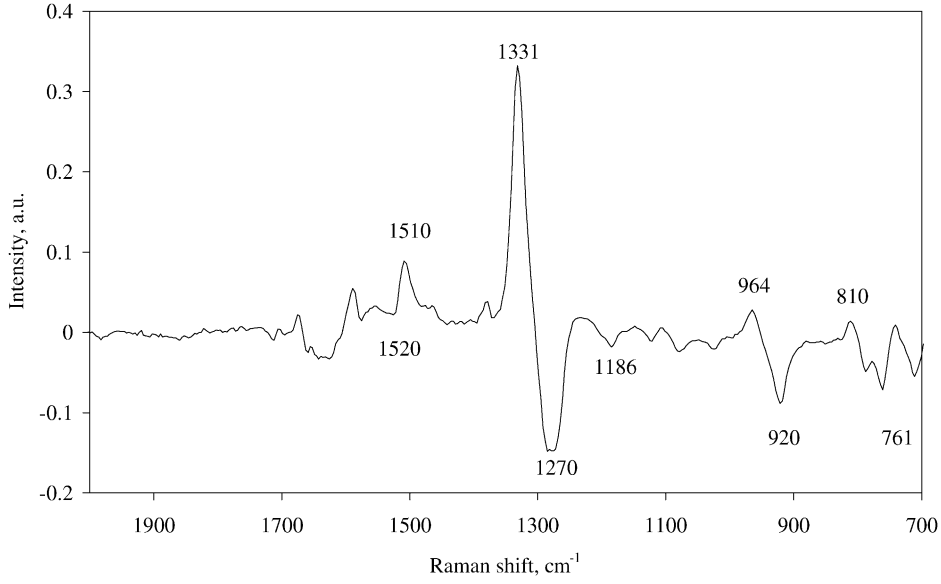

Fig. 3. The loadings line spectrum of the first component of G and S model. Positive bands correspond to S characteristic frequencies and negative bands to G frequencies.

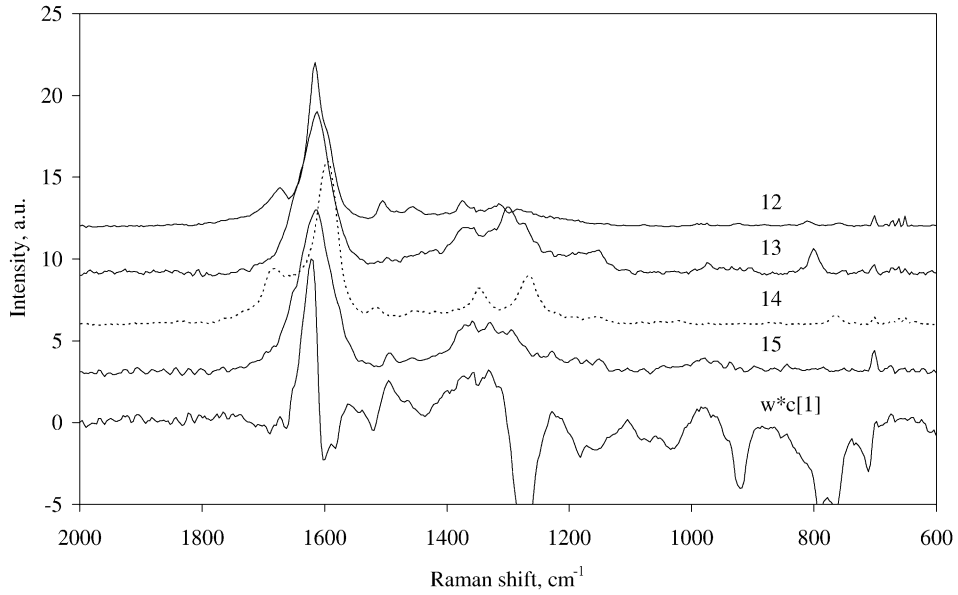

Fig. 4. Loadings line spectrum and UVRR spectra (257 nm) of C5 condensed structures. The numbers refer to model compound numbers depicted in Fig. 1. Note that the degree of condensation varies in the model compounds and is 0% for the model compound presented with dashed line.

3.1. Monomer type

The feasibility of modeling was initially examined with model compounds representing different aromatic substitution patterns, i.e. *p*-hydroxyphenyl (H), guaiacyl (G) and syringyl (S) structures. The loadings line spectrum (Fig. 3) showed the characteristic vibrational bands of G and S structures which were similar to those assigned earlier by visually comparing the spectra [7]. The model also enables the detection of characteristic Raman bands of low intensity which were not detected visually. The positive bands in Fig. 3 correspond to the characteristic vibrations of S structures whereas the negative bands correspond to G structures.

This example illustrates that the characteristic Raman bands can be elucidated from the loadings line spectra of the PLS models. Hence, the PLS modeling detects the similarities in the given UVRR spectra and thereby indicates that the most important characteristic wavenumber areas that are often very difficult and ambiguous to assign visually. Moreover, the detection of characteristic Raman bands from the UVRR spectra of polymeric lignin samples can be impossible visually whereas PLS models may give more precise information.

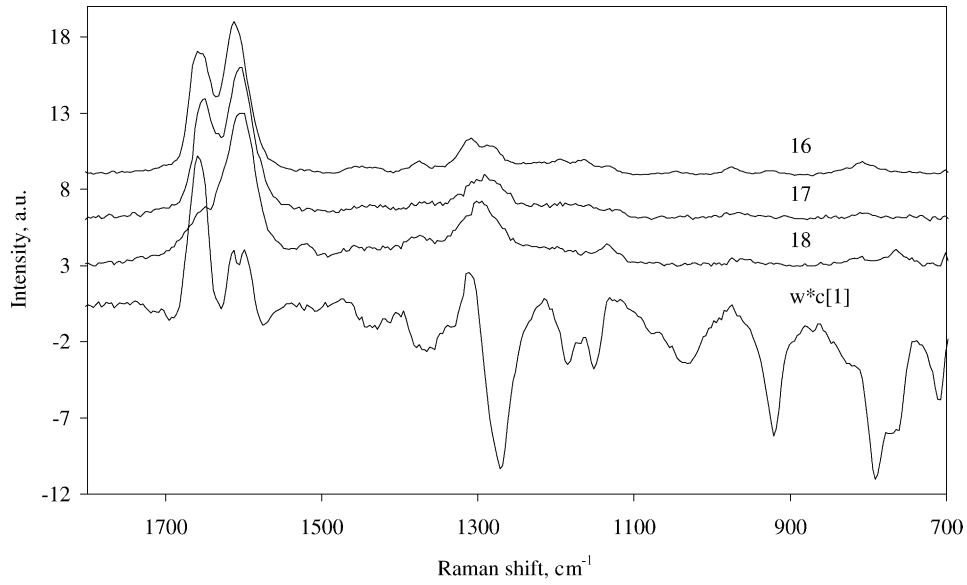

Fig. 5. UVRR spectra (257 nm) of monomeric C=C conjugated model compounds and the loadings line spectrum of their characteristic Raman bands. The numbers refer to model compound numbers depicted in Fig. 1.

3.2. C5 condensed structures

Another model was composed of C5 condensed lignin moieties with varying degrees of condensation. The first component of the model showed the characteristics of the condensed structures as illustrated in the loadings line spectrum in Fig. 4 together with the UVRR spectra of the condensed lignin model compounds (the model compound, which UVRR spectrum is presented with dashed line, has a degree of condensation of 0%). According to the loadings line spectrum, the C5 condensed structures can be characterized at wavenumbers of 1492, 1375–1355, 1328, 1223, 975 cm^{-1}. The Raman band at 1604 cm^{-1} is broadened and therefore, the loadings line spectrum shows two characteristic vibrations at 1618 and 1558 cm^{-1}.

3.3. C=C conjugated structures

3.3.1. Monomers

Monomeric conjugated guaiacyl lignin model compounds were modeled together with non-conjugated guaiacyl structures (compounds **6** and **8** were excluded from the model because they contain a conjugated carbonyl group). The loadings line spectrum of the first component showed characteristic Raman bands of C=C conjugated monomers (compounds **16**–**18**) in the positive direction (Fig. 5, the lowest spectrum). The negative direction corresponds to non-conjugated guaiacyl structures. The loadings line spectrum of the conjugated guaiacyl monomers was compared with the UVRR spectra of these model compounds (Fig. 5). The most prominent Raman band of C=C conjugated monomers is the stretching mode of C=C double bond at about 1658 cm^{-1}. Another important region is found at 1305−1315 cm^{-1}. The respective band is extended to lower wavelengths (1270 cm^{-1}) but that area is even more important for non-conjugated guaiacyl structures as can be seen from the loadings line spectrum. Indeed, the intensity of the Raman band at 1270 cm^{-1} is higher in non-conjugated guaiacyl structures which is also evident from the UVRR spectra of these model compounds (UVRR spectra are presented in [7]). Hence, this region cannot be used in the characterization of conjugation. The band at 1270 cm^{-1} has been assigned to aromatic ether structure [16] that is found both in conjugated and non-conjugated monomers as a methoxyl group attached to C3 carbon. The loadings line spectrum also contains few low intensity bands.

3.3.2. Dimeric conjugated structures

Stilbenes showed characteristic vibrations in the loadings line spectrum of the second component. The model contained C5 condensed and conjugated model compounds (groups B and C). The comparison of the loadings line spectrum with the UVRR spectra of two stilbene model compounds is shown in Fig. 6. The stilbene spectrum was negative in sign but was transformed into positive bands in Fig. 6. The characteristic vibrations of stilbene structures are found at 1638, 1515, 1435–1421, 1263, 1191, 877 and 768 cm^{-1}. The UVRR spectrum of a benzophenone (compound **14**) was very similar to those of stilbene model compounds at wavenumbers below 1600 cm^{-1}. The similarity of the UVRR spectra was also indicated in the scores scatter plot (not shown) in which the benzophenone was grouped close to the stilbene model compounds (**19** and **20**). The structures indeed are rather similar containing two aromatic nuclei and an unsaturated bond conjugated with

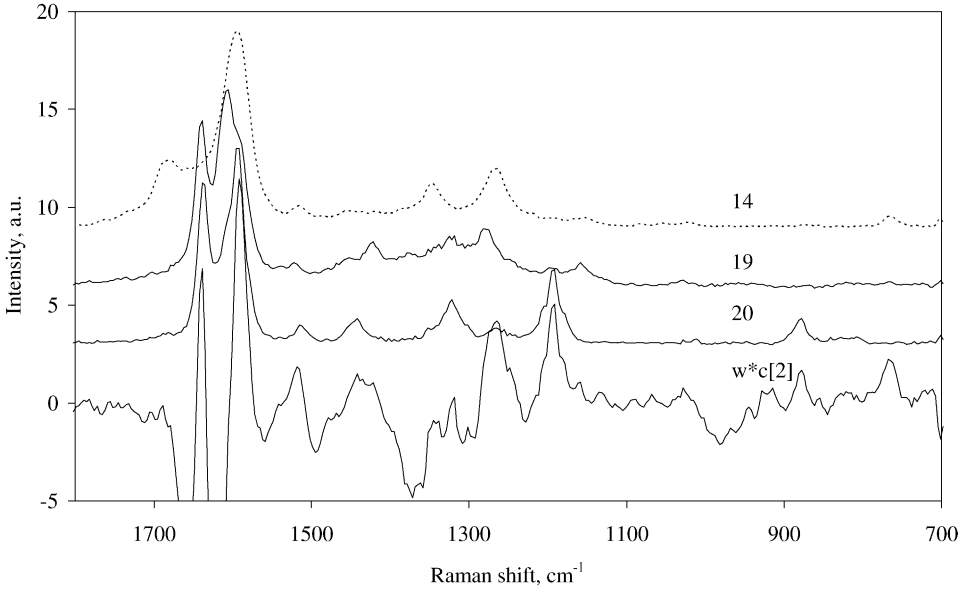

Fig. 6. Characteristic Raman vibrations of stilbene structures presented as a loadings line spectrum (the lowest spectrum) together with the UVRR spectra (257 nm) of two stilbene model compounds (two spectra in the middle) and benzophenone model compound (uppermost spectrum). The numbers refer to model compound numbers depicted in Fig. 1.

both nuclei. The major difference in the spectra was found in the unsaturated stretching region [17]: carbonyl group showed an intensive and characteristic band at the 1683 cm^{-1}, whereas the C=C unsaturated structure had the Raman band at 1638 cm^{-1}.

3.4. C=O structures

Assignment of carbonyl bands in Raman spectroscopy of lignin is rather ambiguous. Firstly, their intensity in general is rather low in comparison with the corresponding IR absorption intensities [17]. In fact, the stretching of the polar C=O group is very strong in IR spectroscopy making it a most sensitive method for detecting trace amounts of carbonyl moieties. Raman spectroscopy can also detect C=O bonds but only at higher concentrations. However, the carbonyl groups conjugated with the aromatic ring absorb light at ~250 nm [18] and therefore, UVRR spectroscopy should also be relatively sensitive tool for detecting carbonyls in lignin due to the resonance effect. Indeed, the stretching mode of C=O bond is easily detected in the UVRR spectra of lignin model compounds (e.g. Fig. 7). The model compounds containing a carbonyl group (compounds **2**, **4**, **6**, **8** and **10**) were grouped in the first component in a PLS model containing all of the 14 monomeric model compounds. According to the loadings line spectrum of the first component (shown in Fig. 7), the carbonyl band is detected at 1688 cm^{-1}. However, the C=O stretching mode in the UVRR spectra of carbonyl containing monomeric model compounds is detected in a rather wide range of 1660–1700 cm^{-1} as shown in Fig. 7. It is thus evident, that the position of the carbonyl band varies significantly depending on its chemical environment.

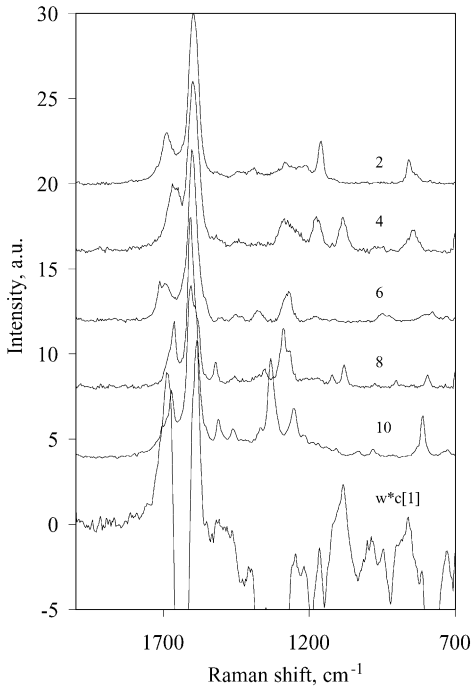

Fig. 7. The loadings line spectrum of the conjugated carbonyl groups and the UVRR spectra (257 nm) of carbonyl group containing monomeric model compounds. The numbers refer to model compound numbers depicted in Fig. 1.

The ambiguity of the interpretation of the stretching mode of unsaturated bonds is evident. The conjugated carbonyl groups present in the lignin polymer have been assigned to the IR band at ~1660 cm^{-1} [19]. Non-conjugated and conjugated aldehydes absorb IR light at ~1720 cm^{-1} [19]. Contrarily to this, Kihara et al. [20] showed that the C=O stretching would appear at 1620 cm^{-1} when studied with NIR-FT-Raman spectroscopy and the band at 1660 cm^{-1} would be due to conjugated C=C structures. Agarwal et al. [8] proposed that the band at ~1660 cm^{-1} would originate from ring-conjugated C=C and C=O stretch of coniferaldehyde-type lignin, whereas the band at 1620 cm^{-1} would be due to ring-conjugated C=C stretch of the coniferaldehyde structures. It is, however, a well-known fact that the chemical environment and the physical state of the sample can shift the band significantly so that the carbonyl stretching band can be located anywhere between 1720 and 1620 cm^{-1} depending on the nature of the neighboring structures [17]. Hence, the direct differentiation between C=O and C=C structures might be rather difficult with resonance Raman spectroscopy, especially with complex samples such as lignin polymers. Indeed, it is probably necessary to use some chemical methods, such as reduction of carbonyls with sodium borohydride ($NaBH_4$) [21], in order to obtain information on these structures separately.

It cannot be emphasized enough, that conventional IR spectroscopy is certainly a more effective tool to detect carbonyls although their resonance in the UV region may give a possibility to also detect them with Raman techniques. Conventional Raman spectroscopic techniques (excitation in NIR or visible region) are not as sensitive towards carbonyl structures. Alternatively, C=C structures are more easily detected with Raman techniques than with IR spectroscopy. This fact might also be utilized in order to get selective information on these structures: Raman techniques should be used for the determination of C=C structures, whereas IR spectroscopy for C=O structures.

3.5. Characteristic Raman vibrations of different lignin structures

All the sub-structures of lignin model compounds studied and their characteristic Raman vibrations are listed in Table 2. It is noteworthy that some of the vibrations are partly overlapping and the visual elucidation would be hence ambiguous in the interpretation of real lignin samples. Moreover, the complex nature of polymeric lignin samples may broaden the signals and make the interpretation even more difficult. Therefore, the utilization of multivariate data analytical approach in the interpretation of the Raman spectra can be very informative and it may bring a totally new way of studying Raman spectra in details. Some of the

Table 2
Characteristic Raman bands of different lignin structures

Structure type	Characteristic Raman bands (cm^{-1})
p-Hydroxyphenyl	1488, 1405, 1338, 1215[a], 1164[a], 1094, 861–841[a], 644[a]
Guaiacyl	1520[a], 1285–1270[a], 1186[a], 1124, 1078, 1024, 920[a], 784[a], 761[a], 711
Syringyl	1588, 1510[a], 1331[a], 1228, 1148, 1108, 964[a], 810[a], 741
C5 condensed	1618[b], 1558[b], 1492, 1375–1355, 1328, 1223, 975
C=C conjugated monomers	1658, 1538, 1475, 1311, 1215, 1130–1114, 974
Stilbene	1638, 1515, 1435–1421, 1263, 1191, 877, 768
C=O conjugated monomers	1695–1662, 1084

[a] This band was also detected in [7] by visually comparing the spectra of model compounds.
[b] This is not a distinctive band. It is rather a broadening of the Raman band at 1604 cm^{-1}.

small intensity bands in Table 2 could actually be ghost peaks that may appear in the loadings line spectra due to the frequency shifts in different model compounds. Hence, great caution should be paid if small intensity bands are interpreted in more detail or used for characterization purposes. However, small intensity bands are also listed in Table 2 because distinguishing between ghost and real peaks of low intensity is non-specific.

4. Conclusions

The PLS modeling was successfully applied for the interpretation of UVRR spectra of lignin model compounds. The loadings line spectra of selected components showed the characteristic wavelengths of each lignin structure which can be further utilized in the interpretation of the UVRR spectra of polymeric lignin samples. The UVRR spectra of polymeric lignin samples have usually broad signals and the multivariate data analytical approach could be very useful in the characterization of the chemical structure of lignin samples. Only most prominent loadings line spectra (1st or 2nd components) were presented in this paper but minor components may also carry important information about these structures. Those minor components should be taken into account when this modeling is further used in predicting these lignin structures in polymeric lignin samples. The minor components are important if the modeling is used to quantify these structures but not as important if the model is used for the interpretation of the UVRR spectra. The most prominent components give bands that are the most important and most easily detected in the UVRR spectra.

However, a wide variability in the appearance of the stretching mode of conjugated double bonds makes their analysis difficult. PLS modeling may not help much in their characterization because the models interpret the UVRR spectra according to the loadings line spectra. Hence, any changes in the chemical environment of conjugated double bonds shift the stretching frequency significantly and PLS model would not detect the bonds in different environments easily. However, it is possible to create a model that would detect the different environments of the examined samples but known the fact that polymeric lignin samples are so complex, the analysis would not be straightforward.

Having one difficulty in the interpretation of conjugated double bonds, the PLS models seem to work very well for other structures. Further development of such models may allow new analytical possibilities in the characterization of polymeric lignin samples. Indeed, the quantification of these lignin structures could also be possible by further development of PLS models. The approach of using known lignin samples would be relatively straightforward and should be easy to adopt for the lignin analysis. There is, however, lack of reference analytical methods. For example, conjugated C=C bonds cannot be analyzed directly from polymeric lignin samples. Moreover, many of the other analytical methods correlate relatively poorly with each other and hence, the real quantities of different structures in lignin samples are difficult to judge.

Acknowledgements

This work was funded by the National Technology Agency (TEKES), the Academy of Finland and industrial partners (Andritz, Metso, M-real, Stora Enso, UPM-Kymmene). Mrs. Rita Hatakka is acknowledged for her skillful experimental work with the UVRR measurements.

References

[1] C.W. Dence, S.Y. Lin, in: S.Y. Lin, C.W. Dence (Eds.), Methods in Lignin Chemistry, Springer-Verlag, Berlin, 1992, pp. 3–19.
[2] G. Brunow, K. Lundquist, G. Gellerstedt, in: E. Sjöström, R. Alén (Eds.), Analytical Methods in Wood Chemistry, Pulping and Papermaking, Springer-Verlag, Berlin, 1999, pp. 77–124.
[3] M. Halttunen, J. Vyörykkä, B. Hortling, T. Tamminen, D. Batchelder, A. Zimmermann, T. Vuorinen, Holzforschung 55 (2001) 631–638.
[4] A.-M. Perander, M. Halttunen, A.-S. Jääskeläinen, J. Vyörykkä, T. Vuorinen, in: Proceedings of the 11th International Symposium on Wood and Pulping Chemistry, Nice, France, 2001, pp. 331–334.
[5] A.-M. Saariaho, B. Hortling, A.-S. Jääskeläinen, T. Tamminen, T. Vuorinen, J. Pulp Pap. Sci. 29 (11) (2003) 363–370.
[6] H.H. Willard, L.L. Merritt Jr., J.A. Dean, F.A. Settle Jr., Instrumental Methods of Analysis, Wadsworth, Inc, Belmont, CA, USA, 1988, pp. 321–325.
[7] A.-M. Saariaho, A.-S. Jääskeläinen, M. Nuopponen, T. Vuorinen, Appl. Spectrosc. 57 (1) (2003) 58–66.

[8] U.P. Agarwal, S.A. Ralph, R.H. Atalla, Proceedings of the 9th International Symposium on Wood and Pulping Chemistry, Canadian Pulp Paper Association, Montreal, Canada, 1997, pp. 8-1–8-4 (poster pres.).
[9] H. Martens, T. Naes, Multivariate Calibration, John Wiley & Sons Ltd., UK, 1989.
[10] J. Gierer, N.O. Nilvebrant, J. Wood Chem. Technol. 11 (2) (1991) 171–193.
[11] F. Xi, D.W. Reeve, A.B. McKague, J. Wood Chem. Technol. 16 (1) (1996) 35–46.
[12] K. Von Kratzl, I Wagner, Holzforschung Holzverwertung 24 (3) (1972) 56–61.
[13] B.-H. Yoon, M. Okada, S. Yasuda, N. Terashima, Mokuzai Gakkaishi 25 (4) (1979) 302–307.
[14] H. Xu, Y.-Z. Lai, J. Wood Chem. Technol. 17 (3) (1997) 223–234.
[15] D. Lin-Vien, N.B. Colthup, W.G. Fateley, J.G. Grasselli, The Handbook of Infrared and Raman Characteristic Frequencies of Organic Molecules, Academic Press, San Diego, CA, USA, 1991, pp. 227–304.
[16] D.H. Williams, I. Fleming, Spectroscopic Methods in Organic Chemistry, 5th ed. McGraw-Hill International, Bath, UK, 1995,p. 46.
[17] D. Lin-Vien, N.B. Colthup, W.G. Fateley, J.G. Grasselli, The Handbook of Infrared and Raman Characteristic Frequencies of Organic Molecules, Academic Press, San Diego, CA, USA, 1991, p. 73 and 117.
[18] D.H. Williams, I. Fleming, Spectroscopic Methods in Organic Chemistry, 5th ed. McGraw-Hill Publishing Company, UK, 1995, pp. 1–27.
[19] O. Faix, in: S.Y. Lin, C.W. Dence (Eds.), Methods in Lignin Chemistry, Springer-Verlag, Berlin, 1992, pp. 91–104.
[20] M. Kihara, M. Takayama, H. Wariishi, H. Tanaka, Spectrochim. Acta A 58 (2002) 2213–2221.
[21] J. Marton, Tappi 47 (1964) 713–715.